Solution Blow Spinning of Piezoelectric Nanofiber Mat for Detecting Mechanical and Acoustic Signals

Eman Elnabawy[1], Mazen Farag[1], Amira Soliman[1], Kamal Mahmoud[1],Nader Shehata[1, 2, 3, 4], Remya Nair[4], Ishac Kandas[1,2,4], RasheedAatif[5], Madeleine Combrinck[5], Jibran Khaliq[5], Islam Shyha[5], Ali Kilic[6,7],Ahmed H. Hassanin[1,8,9*]

[1]Center of Smart Materials Nanotechnology and Photonics (CSMNP), SmartCI Research Center, Alexandria University, Alexandria 21544, Egypt

[2]Department of Engineering Mathematics and Physics, Faculty of Engineering, Alexandria University,Alexandria 21544, Egypt

[3]USTAR Bio innovationsCenter, Faculty of Science, Utah State University, Logan, Utah 84341, United States

[4]Kuwait College of Science and Technology (KCST), Doha District 13133, Kuwait

[5]School of Engineering and the Built Environment, Edinburgh Napier University, Edinburgh EH105DT, Scotland, United Kingdom.

[6]TEMAG Labs, Textile Technology and Design Faculty, Istanbul Technical University, Istanbul, Turkey

[7]Areka Advanced Ltd, Istanbul, Turkey

[8]Department of Textile Engineering, Faculty of Engineering, Alexandria University, Alexandria 21544, Egypt

[9]Materials Science & Engineering Department, School of Innovative Design Engineering, Egypt-Japan University of Science and Technology (E-JUST), 179 New Borg El-Arab City, Alexandria 21934, Egypt

* Correspondence:

Abstract

Solution blow spinning (SBS) technique can produce nanofibers (NFs) mat in large scale production. In this work, the SBS was used to fabricate piezoelectric polyvinylidene fluoride (PVDF) nanofiber membranes that can be utilized for energy harvesting applications. The effect of operating air pressure from (2-5 bar) on the surface morphology of the NFshas been studied. The structuralanalysis forcrystalline polymorph β-phase for PVDF powder, casted film, electrospinning and SBS NFs has also been presented with the aid of Fourier-transform infrared spectroscopy (FT-IR) and X-ray diffraction (XRD). Piezoelectric characteristics of PVDF NFs mats were tested by applying impact impulse with different weights from different heightsbetween 1 cm and 10 cm. The sensitivity of the voltage response increased from 1.71 mV/g to 8.98 mV/g respectively. Besides, the SBS generated PVDF mat is found to be sensitive to pressure forces in a range of few Newtons with the generated voltage according to detected sensitivity of 80 mV/N with analysis of the impact of a few Hertz mechanical vibrations. In addition, the produced SBS nanofibers are applied as an acoustic signal detector within different acoustic frequencies. The results prove that the β-phase PVDF nanofibrous membrane produced via the SBS technique has a great potential to be used as a piezoelectric sensor.

Keywords: solution blown, piezoelectric nanofiber, energy harvesting

1. Introduction

Nanofibers have been widely used as a promising material for various applications such as energy[1], textile[2], filtration [3]and biomedical engineering[4]. Up to date, several methods have been utilized for non-woven nanofiber fabrication which includes template synthesis[5], thermal-induced phase separation [6], self-assembly[7], melt spinning[8], centrifugal force spinning [9] and electrospinning [10]. Electrospinning is considered to be the most common, versatile and cost-effective technique for nanofiber production [11]. Despite these advantages, there are several limitations for needle electrospinning type, such asthe required high electric voltage, low production rate, difficulty to obtain 3D structure andrepeatability challenge [12].This demands either improvements, with potential large investment, to the existing electrospinning systems or the development of alternative techniques.

SBS became a promising technology for nanofiber synthesis due to its low cost, higher production rate (compared to electrospinning) and simplicity of the setup[13, 14]. SBS as a novel technique for nanofiber scaling-up production to make non-woven webs with fiber diameters like those produced by electrospinning. Medeiroset al.[15] first developed SBS methodin which they combined solution blowing and melt blowing techniques involving extruding molten polymer through a narrow orifice directly into a stream of ahigh-velocity hot air which elongates the molten polymer into fibres[16]. The setup for SBSconsists of a nozzle with unique concentric design through which the polymer solution is ejectedby the action of either an inert gas(e. g. nitrogen, argon) or air that in turn allows quick solvents evaporation[17]. This process usually produces randomnon-woven mats comprising micro or nanofibers. Fibres using thermoplastic polymers such as polyetheneoxide (PEO), polyurethane (PU) and polyvinylidene fluoride (PVDF) were successfully manufacturedusing SBS technique [13, 18-20] for potential applications in biomedical and electricalindustries. Using SBS, not only fibres of pure polymers can be produced, but polymer-ceramic composites can also bemade [21].

The filtration efficiency of the NFsmat produced by SBS ranged from 83.10 % to 93.45 %, and the pressure drop was between 15.37 and 30.35 Pawhich is hugely lower than the reported data for electrospun and commercial membranes. Nylon 6 air filtration membrane was made through SBS technique with studying the membrane properties such as thickness and pore size on the filtration performance [16]. Furthermore, PVDF/Ni composite NFs were produced from the SBS method with superior magnetic properties [19]. The magnetic analysis of the nanocomposite showed that it has the same behaviouras ferromagneticmaterials. At the same time, the zero-field cooling (ZFC) and field cooling (FC) curves revealed the presence of super paramagnetic performance which makes it suitable for various applications such as electric motors and generators. Combined nanofiber fabrication methods via electrospinning and solution blowing were introduced to produce self-powered non-woven nanogenerator that can be used in wearable electronic textiles[22, 23]. The design of nanogenerator system consisted of flexible and conductive PVA/PEDOT: PSS mat prepared by electrospinning and working as an electrode, while the second layer was the piezoelectric PVDF nanofiber which was prepared by SBS with the aid of high-pressure airflow. Thepiezoelectric properties showedhigh negative and positive output current of70 nA and−65 nA at an impact frequency of 3 Hz with highdurability and robustness, which proves the capability of a nanocomposite structure in wearable electronics and energy harvesting applications.

In this study, we have used a facile technique for producing PVDF nanofibers membrane for piezoelectric applications employing bespoke concentric SBS nozzle system. The preliminary tests aimed to obtaina highlyefficient piezoelectric response from theSBSmat using different operating air pressures and studying their effect on the morphological structure of SBS nanofibers. A detailed comparison for the structural properties of PVDF powder, cast film, electrospinning and SBS has been investigatedthrough the FTIR and XRD analysis. As an application, our SBS mat was analysed to detect mechanical vibrations of a few Hz frequency range. In addition, the developed nanofibers membranes were applied as an acoustic signals detector at different acoustic spectrum frequencies.

2. Materials and Methods

2.1 Materials

PVDF (Kynar, melt viscosity: 23.0-29.0) was supplied byARKEMA(King of Prussia, PA, USA). N, N-Dimethyl Formamide (anhydrous, 98%) is purchased from LobaChemie (India). Chemicals have been used without further dilution or purifications.

2.2 Nanofibers membrane manufacturing

A custom-made SBS concentric nozzle is provided by AREKA group, Turkey for nanofiber production. Air pressures of 2, 3, 4, and 5 barusing (Cruiser air compressor, 30L, 1.5 HP, China)is used to study the effect of air pressure on the morphological structure of PVDF nanofibers.15 wt. % of PVDF polymer solution is pumped with the aid of NE-300 infusion syringe pump on10 ml/h flow-rate through a 21-gauge needle, which is located inside the concentric nozzle with internal diameter d_i = 2 mm at a working distance of 30cm between the nozzle and drum collector (Figure. 1)[24]. Electrospun PVDF nanofiber and casted film were manufactured to compare the difference in the crystalline phases between the PVDF structures (Powder, Electrospun NF, Solution blown NF, and casted membrane). The electrospinning process was performed using NE1000 syringe pump (New Era Pump Systems, Suffolk County, NY, USA) to control the flow rate at 1 ml h^{-1} at 25 kV through a high-voltage power supply CZE1000R (Spellman, Hauppauge, NY, USA). A grounded rotating drum collector at 1000 rpm is placed 10 cm away from the needle tip to collect the PVDF nanofibers. The casted membrane was produced using the vapour induced phase separation (VIPS) technique.

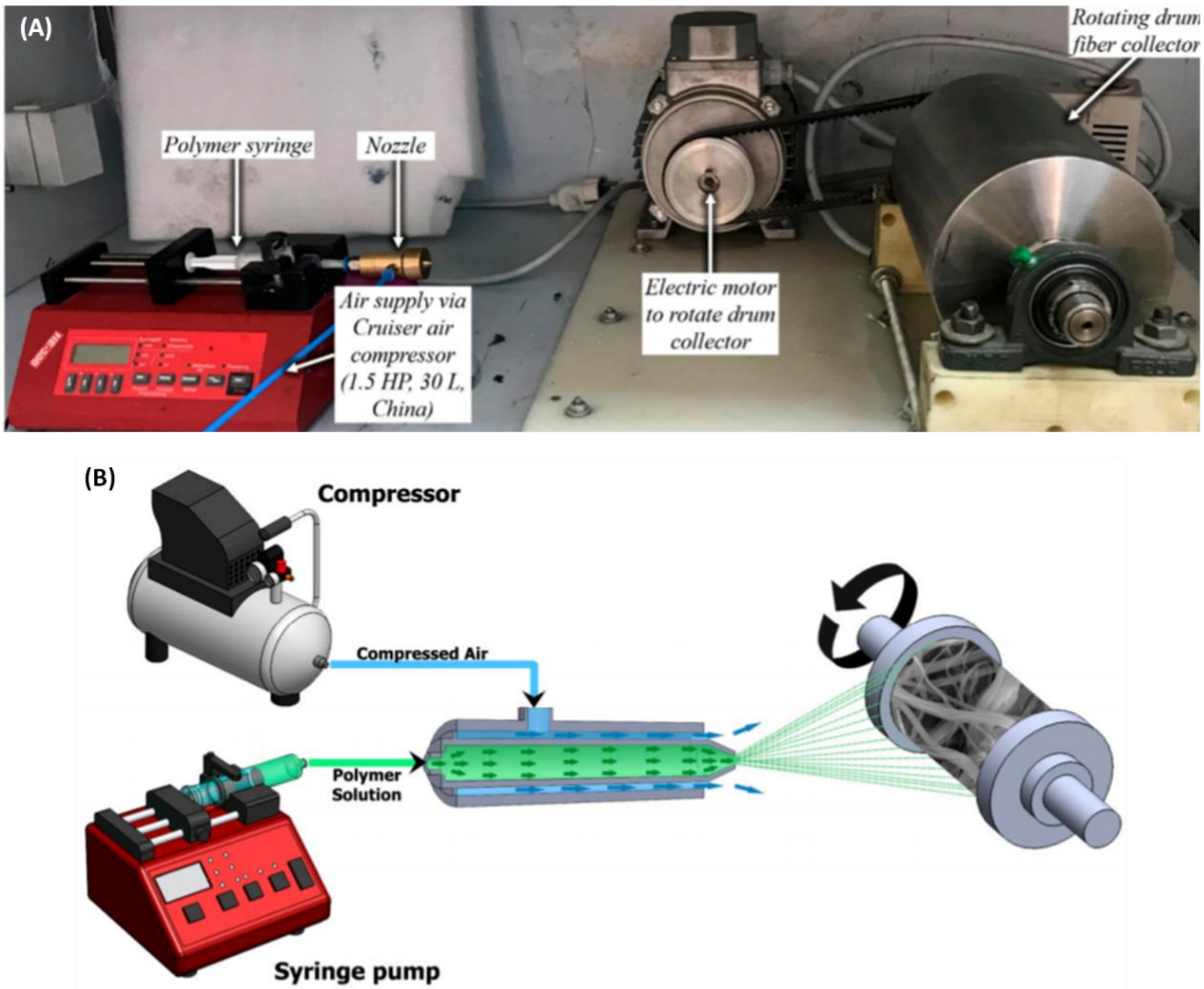

Figure 1: (A) Image of solution blow spinning set up and, (B) Schematic description of the process

2.3Material Characterization

2.3.1 Fibre morphology

The morphological structure of SBSPVDF NFs has been observed by the Scanning Electron Microscope (JEOL, JSM-6010LV-SEM). One sample for each pressure was cut and stacked onto carbon tabs before sputtering with platinum. The average fibrediameter wasmeasuredusing Image-J softwareatthree different image scales (5 μm, 10 μm and 50 μm).

2.3.2 Physical properties

The crystalline phase of PVDF powder, cast film, electrospinning and SBS NFs was determined using X-Ray Diffractometer (XRD) (Shimadzu Xlab 6100 instrument using Cu as a target), scanning range of 5-80º and scanning speed of 1deg/min for precise detection of the peaks.

Fourier transform infrared spectrometer (FT-IR) (Vertex 70 FT-IR, Bruker, Billerica, MA, USA) was operated in ATR mode. Samples were scanned 120 times at a resolution of 5 cm^{-1} over a range of 4000–400 cm^{-1}.

2.4 Piezoelectric measurements

Piezoelectric properties of the nanofiber mats were measured using two bespoke lab setups.The first one is calledimpulse loading, where the peak-to-peak voltage is detected when letting small masses to freely fall onto the developed nanofibers mats. The nanofibers mat of 2 cm x 2 cm wasplaced between two aluminiumelectrodesand exposed toimpulse loading from heights of 1 cm and 10 cm (Figure 2)[25].The generated voltage wasmeasuredusingtwo shielded wires, pasted on the electrodes, and connected to high impedance mixed domain oscilloscope (Tektronix MDO3012, Beaverton, OR, USA). In the othermeasurementsetup, piezoelectric testing was performed using a tool designed to control the applied force on PVDF nanofibers through a motorized spring. Changing the length of the spring could control the applied force on the piezo nanofibers. The nanofibers mat is inserted between two electrodes and connected through shielded wires to thepreviously mentioned oscilloscope. Then, the peak-to-peak voltage is measuredwith respect to the change in the applied force within sensitive range of few Newtons.

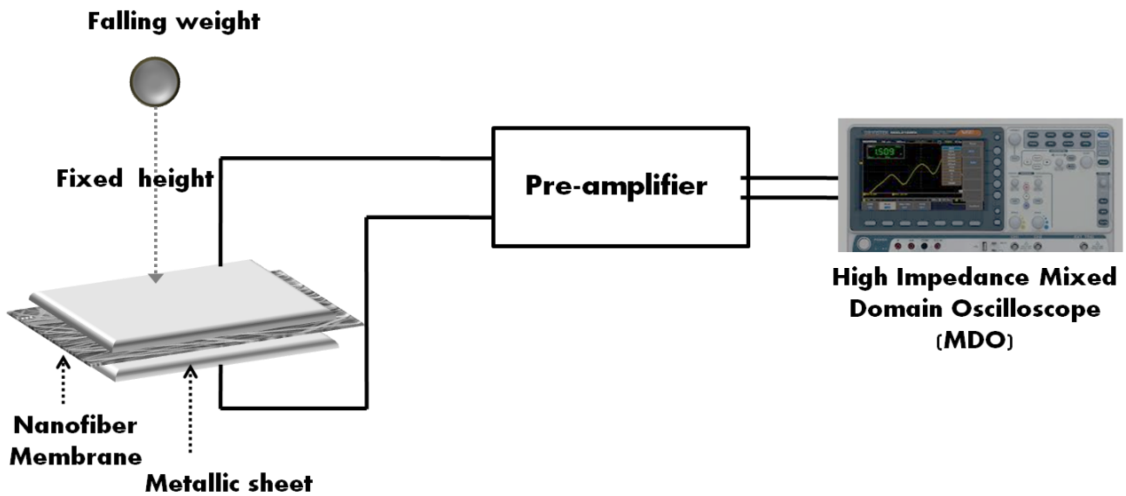

Figure 2. Schematic description of the impulse loading setup

In a modified version of the previously mentioned piezoelectric setup, a source of acoustic signals (Figure 3)[26], which is aTektronix function generatorof Model AFG1062 with frequency range of 60 MHz and sampling rate of 300 MS/s, is connected through an acoustic amplifier to a speaker. Then, the oscilloscope shows the retraced acoustic signals detected by the nanofibers mat.

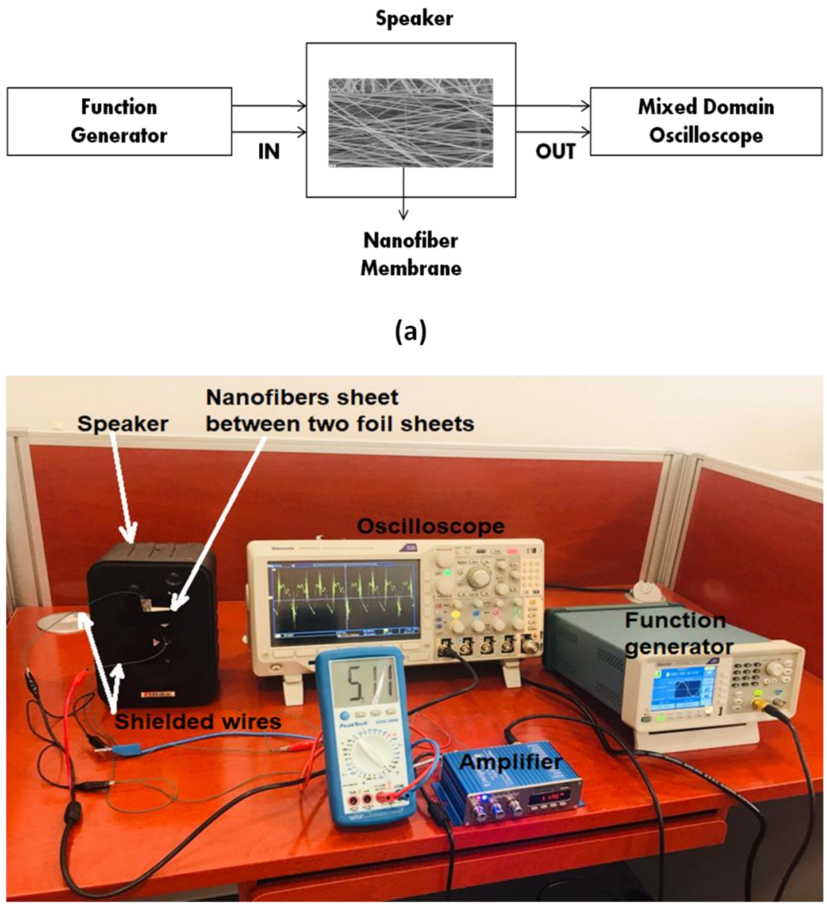

(b)

Figure 3. Schematic diagram of the acoustic energy harvesting setup (a), and a picture of the experimental setup

3.Results and Discussion

3.1 Morphological Characterization

Figure 4 shows SEM images and diameterdistributionsof PVDF NFs produced at different air pressures (2, 3, 4 and 5 bars). Clogging and obstruction of the tip nozzle at 2 and 3 barswere occurred due to the formation and subsequent accumulation of polymer droplets which solidified very quickly, thus producing nanofibers with some distributed beads. To overcome the polymer solidification and increase the solvent evaporation rate, higher operating air pressuresof 4 and 5 barswere applied. As shown in Figure 4(D), stacked bundles were formed with the highest pressure used in this study (5 bar). The produced nanofibers at 4 bars showed the highest quality in terms of homogenous network and smaller fibre diameter distribution in the range of 178 nm without any observed beads or polymer stains. Therefore, these nanofibers produced at 4barswere chosen forpiezoelectric measurements.

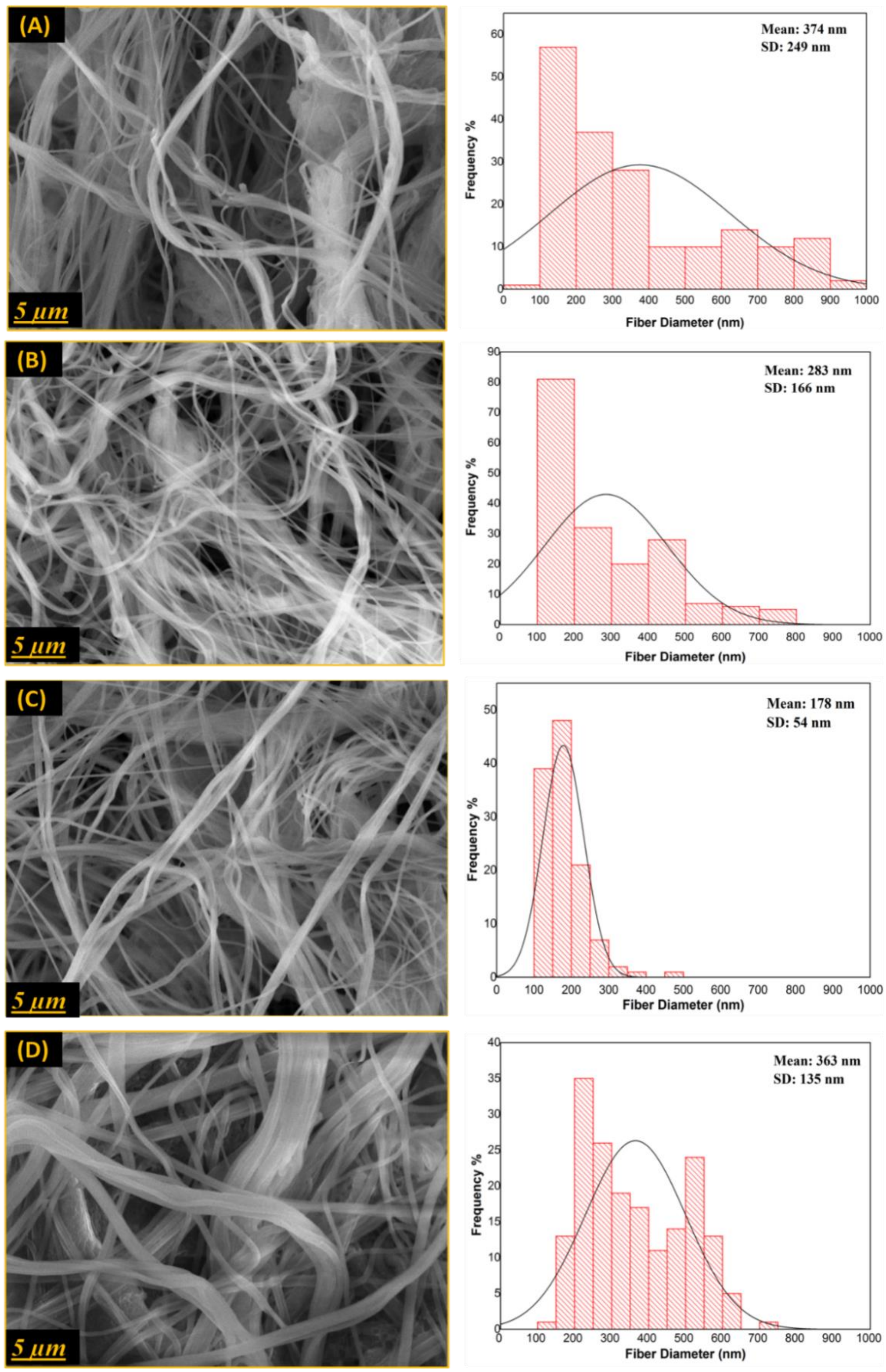

Figure4: SEM images for solution-blownnanofiber produced at different air pressure values (A) 2 bar, (B) 3 bar, (C) 4 bar and (D) 5 bar.

3.2 Structural Characterization

3.2.1 X-ray Diffraction (XRD)

Figure 5 shows the XRD pattern for rawPVDF powder, casted film, electrospun and solution blown NFs. PVDF powder showed two distinct broad peaks at 2Θ = 18.16º and 26.24º and a sharp rise at 2Θ = 19.76º.These peaks are attributed to the reflection of 021, 020, 110, and 200 monoclinic *α*-phase crystalplanes[22, 27, 28]. The casted film showed similar distribution with two intensive peaks at 18.06° and 19.6° which is attributed to the *α* PVDF phase[28, 29]. The *α* phaseof PVDF powder and casted film has low potential energy and non-polar trans gauge conformation (TGTG) structure due to the anti-parallel arrangement of the chains[27]. However, when PVDF was processed using SBS, the PVDF pattern showed a weak shoulder at ~2Θ = 18.06ºdepicting the disappearance of *α* crystalline phase. The peak around 2Θ = 19.76ºwas shifted to 20.64ºwhich is the diffraction peak on planes 110 and 200,indicating enhanced β crystalline phase owing to the transformation from *α* to the β PVDF [22]. The transformation was the result of the alignment of the β phase, all-trans (TTTT) zigzag chain conformation as a consequence of the dipole moment direction which is parallel to the force resulted from the applied air pressurethat stretched PVDF. The dipolesare perpendicular to the polymer chain causing an increase in the dipole moment, which results in high polarization.

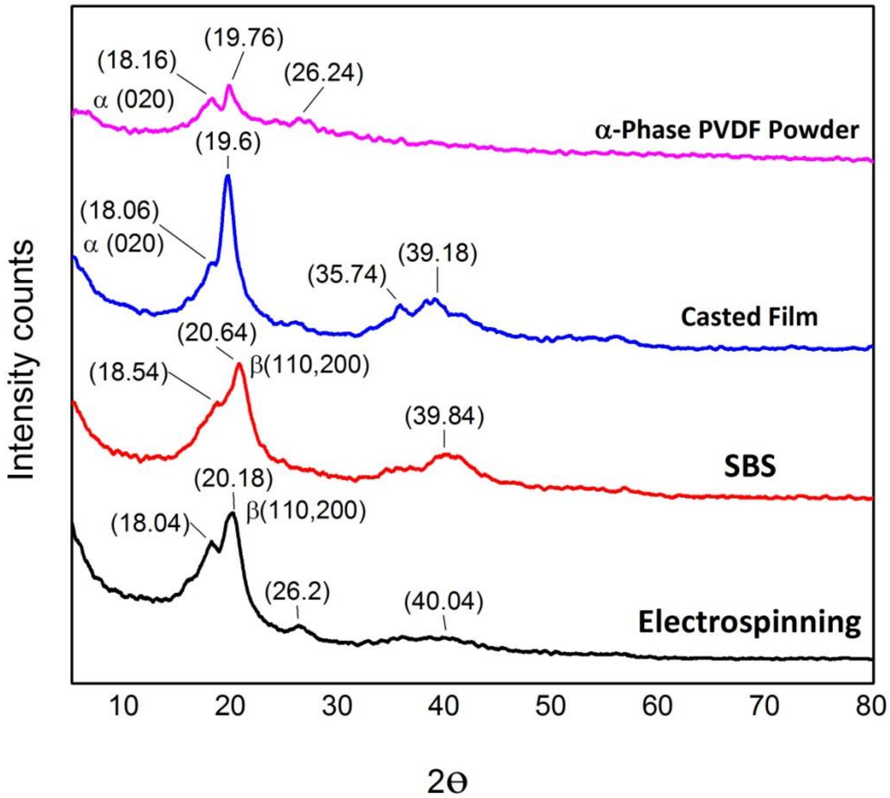

Figure 5: XRD pattern of PVDF powder, cast film, SBS and electrospinning

The crystallinity(β) of PVDF NFs produced by SBS technique can be calculated by the peak deconvolution method from the following equation [30].

$$\beta(\%) = \left(\frac{A(\beta)}{A(\alpha)+A\,(\beta)}\right) \times 100\ \% \qquad (1)$$

Where A_β,A_α are the area under the curves of the βand α,respectively. Origin software was used to calculate the area by the peak integration method as shown in Figure 6a&b.It was found that A_α = 77.4whileA_β =516.9, giving the crystallinity of β phase to be ~ 87%. Table 1 shows the β phase content for the different PVDF crystalline structures.

Table 1: The β phase content for the different PVDF crystalline structures

Sample	Raw powder	Casted film	SBS NFs	Electrospun NFs
β-phase content %	No β Phase	No β Phase	87%	74%

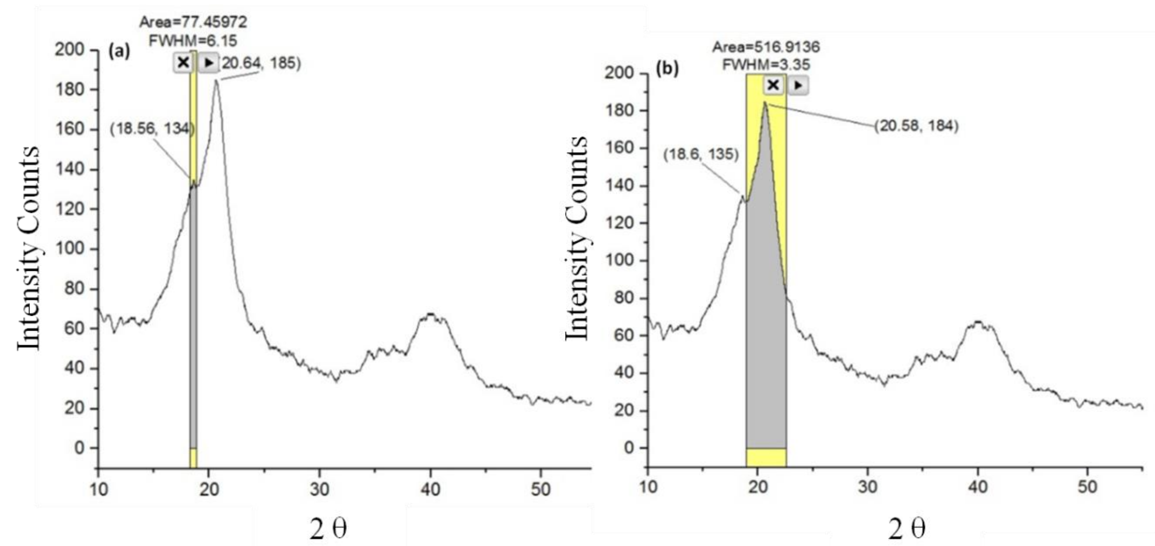

Figure 6: Calculations of areas under (a) alpha, and (b) beta curves of SBS NFs.

3.2.2 FTIR

Figure 7 displays FTIR spectra for thePVDF NFs manufactured through different techniques. Asharp peak was noticed at 763 cm^{-1} for PVDF powder which is indicative of theα phase[31]. The peaks intensity of the α phase, which appeared at 757 cm^{-1} and 761 cm^{-1} for electrospinning and cast PVDF NFs. In contrast, the α phase completely disappeared when using SBS for producing PVDF NFsas corroborated by XRD resultsshown in figure 5. The spectra for PVDF powder show a veryweak peak at ~ 838 cm^{-1}which could be ascribed to the β phase[32]. This peak appeared sharply with higher intensity in PVDF processed through electrospinning, SBS and casting technique. These results are in agreement with the XRD results, as discussed earlier.Figure 8 shows the difference in monomers arrangement between α-PVDF (TGTG) and β-PVDF (TTTT).

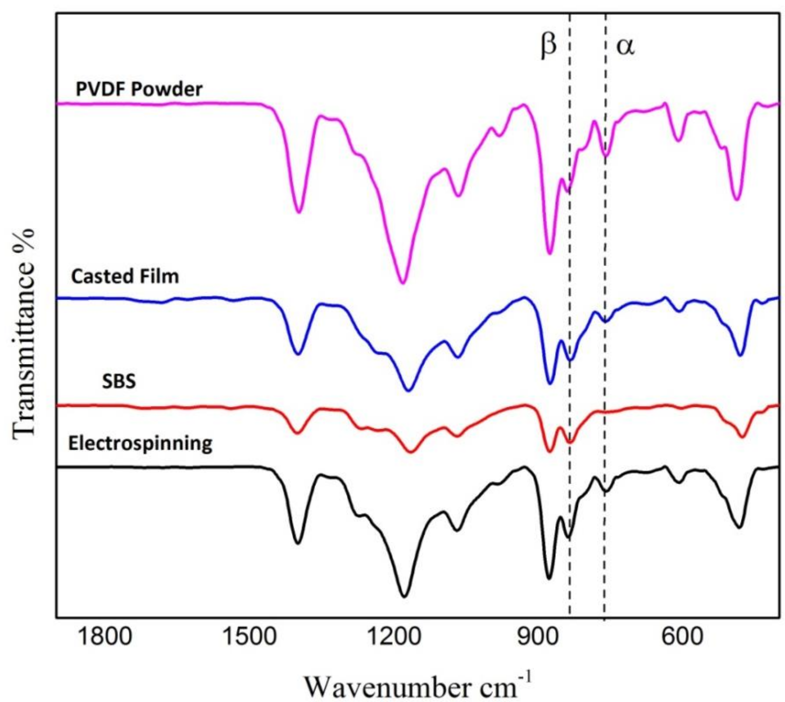

Figure 7: FTIR of PVDF powder, cast film, Solution blown and electrospunnanofibers

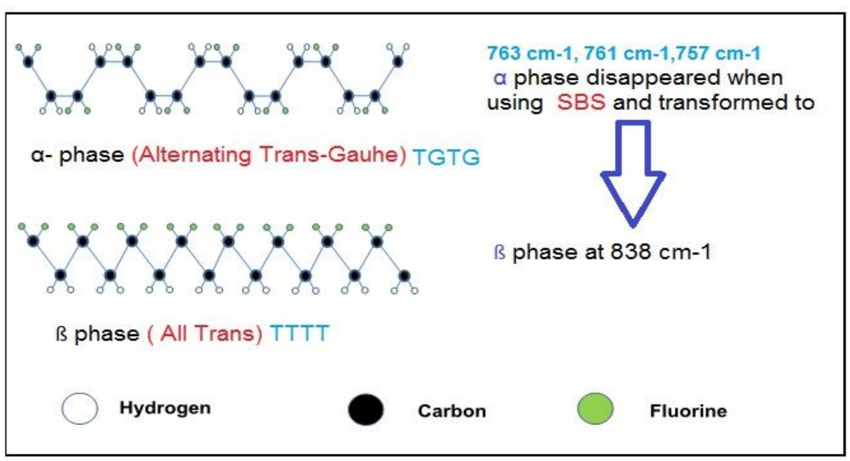

Figure8: The arrangement of monomers in alpha and beta phases of PVDF

3.4 Piezoelectric Measurements

Figure 9shows the piezoelectric response of the SBS NFs mats under impulse loading impact from two different heightsof 1 cm and 10 cm. The generated electric potential response increases with increasing weight. The generated electrical potential within a higher height impulse loading case is higher in both voltage value and sensitivity. The slope between mean peak-to-peak voltage and applied falling masses, which presents the sensitivity response, is found to be 8.98 mV/g in case of 10 cm height of falling masses impulse loading compared to 1.71 mV/g in case of 1 cm height. That indicates the piezoelectric response of our developed nanofibers mats according to impulse forces, with increased sensitivity of voltage conversion in case of incremental impulse force associated to higher falling objects.

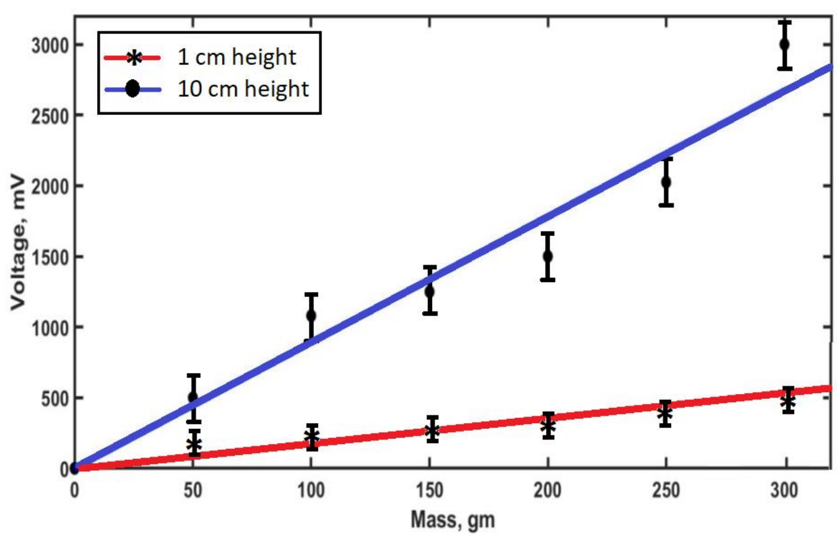

Figure 9: Piezoelectric responses (voltage) of solution blown nanofibers mat at both 1 cm and10 cmimpulse loadingwithdifferent masses.

In another piezoelectric analysis, different applied forces were exposed to the developed PVDF nanofibers mat. Figure 10 shows the generated electric voltage under applied cyclic forces on the SBS nanofibers mat. Figure 11 shows the output peak-to-peak voltage at different applied forces. It can be noticed that the developed nanofibers can be sensitive to a few Newton loads with piezoelectric response sensitivity of 80 mV/Nat cyclic stress of 1 Hz frequency, due to the formed aligned electric dipoles associated to β-sheets inside SBS nanofibers. Further experiments of the impact of cyclic frequency of the applied forces have been verified. Figure 12 shows the relation between generated voltage and the used cyclic forces at different frequencies. At lower frequency of around 1 Hz, the relationship is relatively linear compared to high-frequency mechanical vibrations above 8 Hz. Beyond 8 Hz, there is some linearity of the relationship between voltage and force in particularwithin the region of applied forces, as shown in Figure 13. Overall, the piezoelectric sensitivity, which represents the relation between the applied mechanical forces and the generated electric potential, of the SBS piezoelectric mats is around 350-500 mV/N over the used frequencies with a change in the linearity response or slope according to the applied frequency.

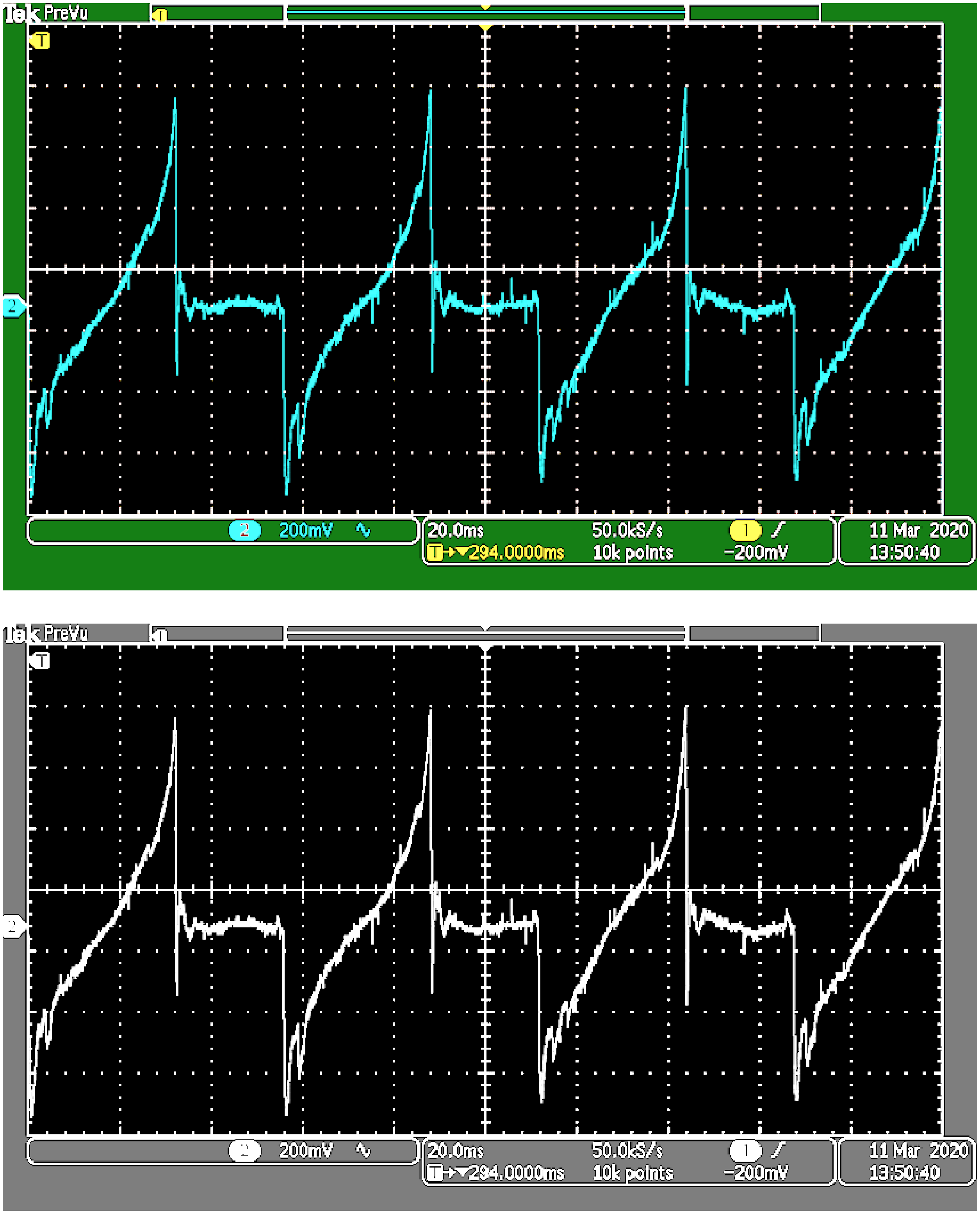

Figure 10: Electric response of SBS nanofibers mat at a cyclic applied force (y-axis represents the generated voltage and x-axis is the time).

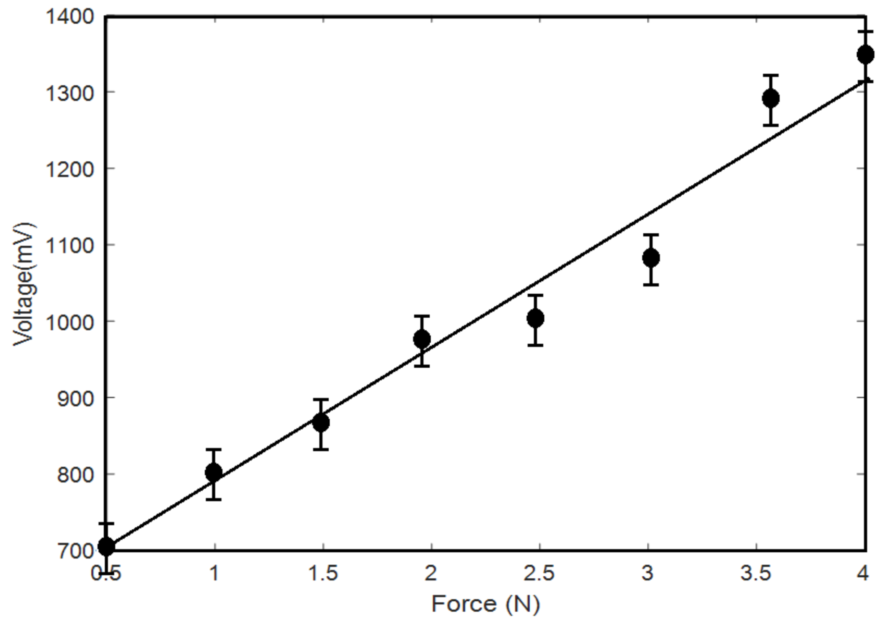

Figure 11. The relation between mean peak-to-peak generated voltage according to different applied forces at 1 Hz.

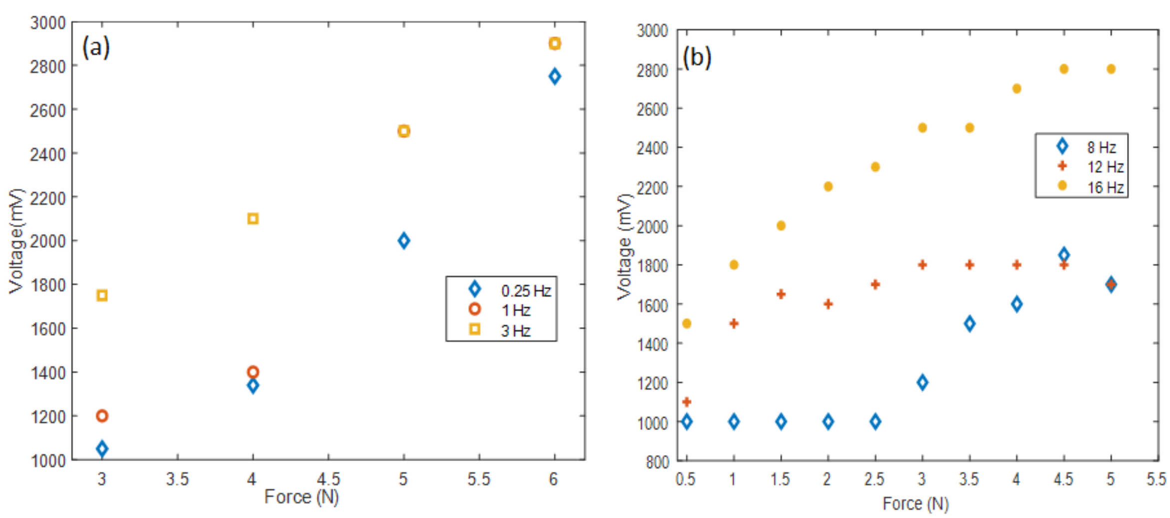

Figure 12. The relation between mean peak-to-peak generated voltage according to different mechanical forces at different frequencies.

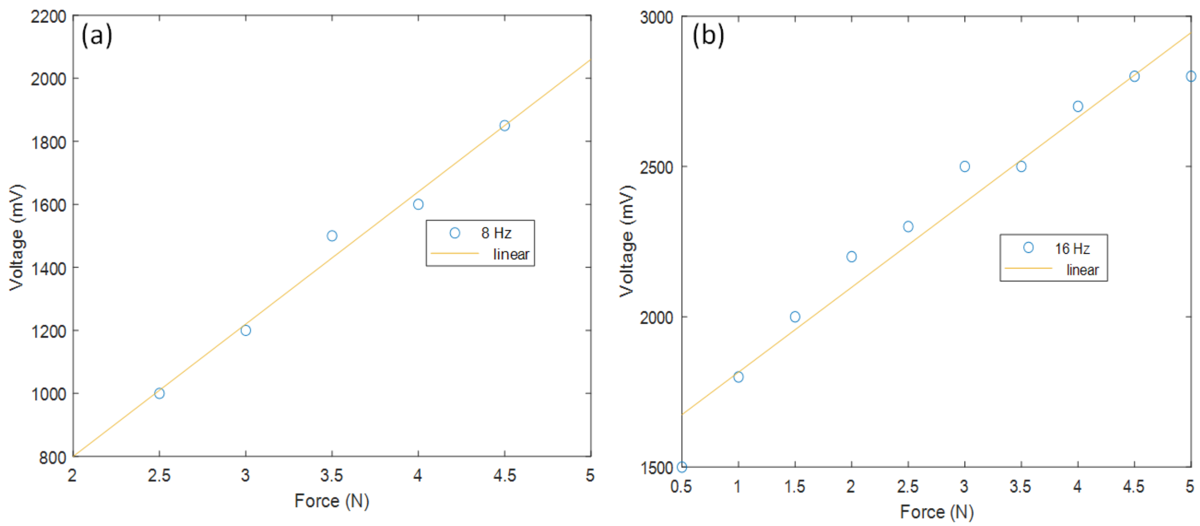

Figure 13. Linear fitting of the relation between generated voltage and cyclic force at (a) 8 Hz and (b) 16 Hz

The developed SBS nanofibers mat was also exposed to a wide range of audio signal frequencies from 100 Hz to 20 kHz, with a wide range of amplitudes up to 6 V. As shown in Figure 14, the output voltage generated from the NFs mat is found to be increasing almost linearly for low applied voltage with an increase in frequency upto 2 kHz. At higher frequencies beyond 5 kHz, there is saturation behaviour in the response of the piezoelectric nanofibers against applied acoustic signals at any of the used amplitudes. Overall, the level of voltage detected is increasing with increased voltage amplitude of the applied acoustic signal.As an example, the detected voltage is plotted against the input acoustic amplitude at an acoustic frequency of 2 kHz in Figure 15. It is found that there is a linear relationship between both output/input voltages with a correlation factor of 30 mV/V.

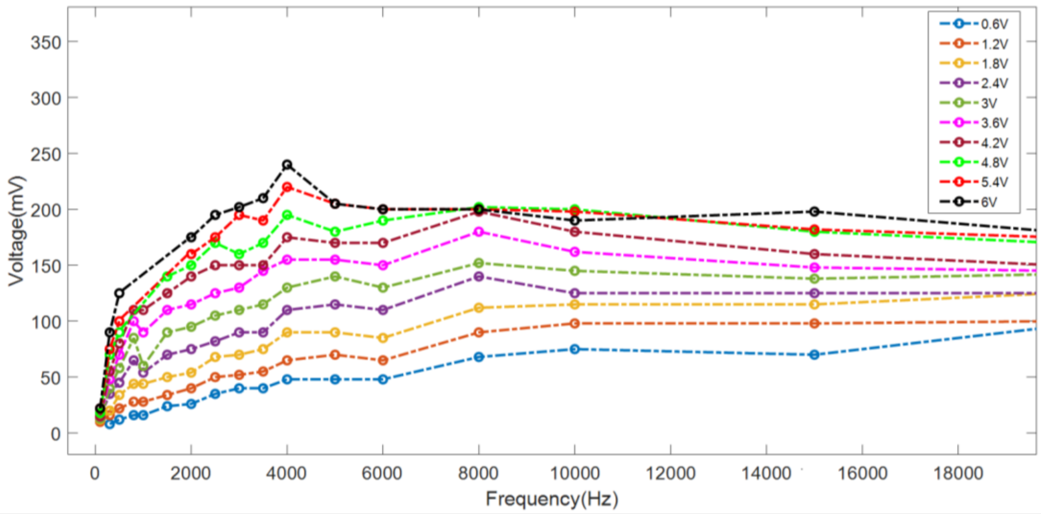

Figure 14. Measured voltage versus frequency at different input applied voltage amplitudes.

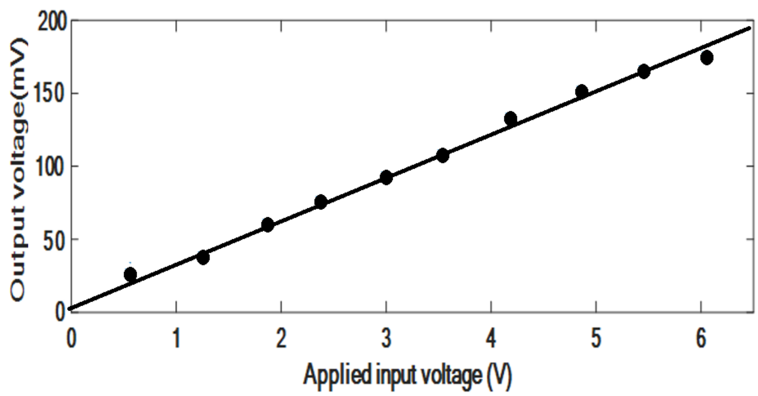

Figure 15. The relation between outputs generated voltage against the amplitude of input acoustic signal at the acoustic frequency of 2 kHz.

Conclusions

Piezoelectric PVDF nanofiber mats were successfully fabricated by a bespoke SBS setup employing a custom-made concentric nozzle. The produced nanofibrous mat showed homogenous diameter distribution in the range of 200nm. At the same time, the formation of β-phase PVDF through SBS and confirmed by XRD and FT-IR analysis led to a noticeable increase in the generated electric potential and sensitivity under different impulse loading up to 8.98 mV/g in case of 10 cm height. Furthermore, the generated SBS nanofiber mats were sensitive to the applied force of only a few Newtons and generated electric signals with a sensitivity of up to 500 mV/N at different applied cyclic vibrational frequencies. As an application to our developed mats, the fabricated SBS nanofiber mats have been used to detect the audio acoustic signals with linear behaviour up to 2 kHz acoustic frequency. All of these results demonstrated that solution blow spinning of PVDF non-woven matswill have several potential applications and can be usedin the large-scale production of energy harvesting devices.

Acknowledgment

The authors would like to thank Science, Technology & Innovation Funding Authority (STIFA) for providing funding for the Institutional Links Project between Alexandria University, Egypt, and Northumbria University, Newcastle upon Tyne, UK. This work is part of the project of (Newton-Mosharafa Call between UK and Egypt, ID: 30886) which has been funded by Science, Technology & Innovation Funding Authority (STIFA), Egypt.

Conflicts of Interest

The authors declare no conflict of interest

References:

1. Abbasipour, M., et al., *Improving piezoelectric and pyroelectric properties of electrospun PVDF nanofibers using nanofillers for energy harvesting application.* Polymers for Advanced Technologies, 2019. **30**(2): p. 279-291.
2. Jin, H., et al., *Highly Durable Nanofiber-Reinforced Elastic Conductors for Skin-Tight Electronic Textiles.* ACS Nano, 2019.
3. Alias, N.H., et al., *Photocatalytic nanofiber-coated alumina hollow fiber membranes for highly efficient oilfield produced water treatment.* Chemical Engineering Journal, 2019. **360**: p. 1437-1446.
4. Nandi, S.K., et al., *Organic–inorganic micro/nanofiber composites for biomedical applications*, in *Materials for Biomedical Engineering*. 2019, Elsevier. p. 21-55.
5. Huang, J., et al., *Polyaniline nanofibers: facile synthesis and chemical sensors.* Journal of the American Chemical Society, 2003. **125**(2): p. 314-315.
6. Nayani, K., et al., *Electrospinning combined with nonsolvent-induced phase separation to fabricate highly porous and hollow submicrometer polymer fibers.* Industrial & Engineering Chemistry Research, 2011. **51**(4): p. 1761-1766.
7. Hartgerink, J.D., E. Beniash, and S.I. Stupp, *Self-assembly and mineralization of peptide-amphiphile nanofibers.* Science, 2001. **294**(5547): p. 1684-1688.
8. Huang, T., et al., *Production of nanofibers by melt spinning*. 2012, Google Patents.
9. Weitz, R., et al., *Polymer nanofibers via nozzle-free centrifugal spinning.* Nano letters, 2008. **8**(4): p. 1187-1191.
10. Huang, Z.-M., et al., *A review on polymer nanofibers by electrospinning and their applications in nanocomposites.* Composites science and technology, 2003. **63**(15): p. 2223-2253.
11. Persano, L., et al., *Industrial upscaling of electrospinning and applications of polymer nanofibers: a review.* Macromolecular materials and engineering, 2013. **298**(5): p. 504-520.
12. Haider, A., S. Haider, and I.-K. Kang, *A comprehensive review summarizing the effect of electrospinning parameters and potential applications of nanofibers in biomedical and biotechnology.* Arabian Journal of Chemistry, 2018. **11**(8): p. 1165-1188.
13. Polat, Y., et al., *Solution blowing of thermoplastic polyurethane nanofibers: A facile method to produce flexible porous materials.* Journal of Applied Polymer Science, 2016. **133**(9).
14. Costa, D.L., et al., *Synthesis of TiO2 and ZnO nano and submicrometric fibers by solution blow spinning.* Materials Letters, 2016. **183**: p. 109-113.
15. Medeiros, E.S., et al., *Solution blow spinning: A new method to produce micro-and nanofibers from polymer solutions.* Journal of applied polymer science, 2009. **113**(4): p. 2322-2330.
16. Shi, L., et al., *Solution blowing nylon 6 nanofiber mats for air filtration.* Fibers and Polymers, 2013. **14**(9): p. 1485-1490.
17. Ho, D.H., et al., *β-Phase-Preferential blow-spun fabrics for wearable triboelectric nanogenerators and textile interactive interface.* Nano Energy, 2020. **77**: p. 105262.

18. Han, W., et al., *Optimization of airflow field via solution blowing for chitosan/PEO nanofiber formation.* Fibers and Polymers, 2017. **18**(8): p. 1554-1560.
19. Dias, Y., et al., *PVDF/Ni fibers synthesis by solution blow spinning technique.* Journal of Materials Science: Materials in Electronics, 2018. **29**(1): p. 514-518.
20. González-Benito, J., et al., *PVDF based nanocomposites produced by solution blow spinning, structure and morphology induced by the presence of MWCNT and their consequences on some properties.* Colloid and Polymer Science, 2019. **297**(7): p. 1105-1118.
21. Daristotle, J.L., et al., *A review of the fundamental principles and applications of solution blow spinning.* ACS applied materials & interfaces, 2016. **8**(51): p. 34951-34963.
22. Liu, R.-Q., et al., *Preparation of Nanofibrous PVDF Membrane by Solution Blow Spinning for Mechanical Energy Harvesting.* Nanomaterials, 2019. **9**(8): p. 1090.
23. Tandon, B., et al., *Fabrication and characterisation of stimuli responsive piezoelectric PVDF and hydroxyapatite-filled PVDF fibrous membranes.* Molecules, 2019. **24**(10): p. 1903.
24. Atif, R., et al., *Solution Blow Spinning of High-Performance Submicron Polyvinylidene Fluoride Fibres: Computational Fluid Mechanics Modelling and Experimental Results.* Polymers, 2020. **12**(5): p. 1140.
25. Elnabawy, E., et al., *Piezoelastic PVDF/TPU nanofibrous composite membrane: Fabrication and characterization.* Polymers, 2019. **11**(10): p. 1634.
26. Shehata, N., et al., *Acoustic Energy Harvesting and Sensing via Electrospun PVDF Nanofiber Membrane.* Sensors, 2020. **20**(11): p. 3111.
27. Mishra, S., et al., *Advances in piezoelectric polymer composites for energy harvesting applications: A systematic review.* Macromolecular Materials and Engineering, 2019. **304**(1): p. 1800463.
28. Abdullah, I.Y., et al., *Facile formation of [beta] poly (vinylidene fluoride) films using the short time annealing process.* Advances in Environmental Biology, 2015. **9**(20 S1): p. 20-28.
29. Su, Q., Z. Jiang, and B. Li, *A mixed solvent approach to make poly (vinylidene fluoride) nanofibers with high β-phase using solution blow spinning.* High Performance Polymers, 2020. **32**(10): p. 1160-1168.
30. Janakiraman, S., et al., *Electroactive poly (vinylidene fluoride) fluoride separator for sodium ion battery with high coulombic efficiency.* Solid State Ionics, 2016. **292**: p. 130-135.
31. Gregorio Jr, R., *Determination of the α, β, and γ crystalline phases of poly (vinylidene fluoride) films prepared at different conditions.* Journal of Applied Polymer Science, 2006. **100**(4): p. 3272-3279.
32. Lin, J., et al., *New potassium sodium niobate/poly (vinylidene fluoride) functional composite films with high dielectric permittivity.* Journal of Polymer research, 2016. **23**(8): p. 152.